Marine Pollution Bulletin 163 (2021) 111934

Contents lists available at ScienceDirect

Marine Pollution Bulletin

journal homepage: www.elsevier.com/locate/marpolbul

Large-scale basin testing to simulate realistic oil droplet distributions from subsea release of oil and the effect of subsea dispersant injection

Per Johan Brandvik [a,*], Emlyn Davies [a], Frode Leirvik [a], Øistein Johansen [a], Randy Belore [b]

[a] SINTEF Ocean, Marine Environmental Technology, Trondheim, Norway
[b] SL Ross Environmental Research Ltd., Ottawa, Ontario, Canada

ARTICLE INFO

Keywords:
Subsea release
Dispersant
Oil
Droplet formation
Modelling
Prediction
Modified Weber

ABSTRACT

Small-scale experiments performed at SINTEF, Norway in 2011–12 led to the development of a modified Weber scaling algorithm. The algorithm predicts initial oil droplet sizes (d_{50}) from a subsea oil and gas blowout. It was quickly implemented in a high number of operational oil spill models used to predict fate and effect of subsea oil releases both in academia and in the oil industry.

This paper presents experimental data from large-scale experiments generating oil droplet data in a more realistic multi-millimeter size range for a subsea blow-out. This new data shows a very high correlation with predictions from the modified Weber scaling algorithm both for untreated oil and oil treated by dispersant injection.

This finding is opposed to earlier studies predicting significantly smaller droplets, using a similar approach for estimating droplet sizes, but with calibration coefficients that we mean are not representative of the turbulence present in such releases.

1. Introduction

The size distribution of oil droplets formed during oil and gas blowouts is known to have a strong impact on the subsequent fate of the oil in the environment (Johansen, 2003; Chen and Yapa, 2003; Zheng et al., 2003). Reliable predictions of size distribution in blowouts will thus improve our ability to forecast the fate of oil in the environment, and subsequently provide better guidance for oil spill response operations and relevant information to the public.

Since the Deepwater Horizon (DWH) spill in 2010, multiple models have been developed to describe oil droplet formation and predict size distributions resulting from a subsea oil and gas blowout (Paris et al., 2012; Johansen et al., 2013; Zhao et al., 2014; Nissanka and Yapa, 2016; Li et al., 2017; Malone et al., 2019; Pesch et al., 2019). Several studies compare selections of these models (Socolofsky et al., 2015; Dissanayake, et al., 2018; Nissanka and Yapa, 2018), but the most complete comparisons are offered by NASEM (2019) and Cooper et al. (2020).

Small-scale experiments performed at SINTEFs Tower basin in 2011–12 led to the development of a modified Weber scaling algorithm (Johansen et al., 2013). It was quickly implemented in a high number of operational oil spill models used to predict fate and effect of subsea oil releases both in academia and in the oil industry (Socolofsky et al., 2015).

The ideal facility for simulation of subsea releases and dispersant injection should hold a large water volume (>500 m^3) with a depth in the 12- to15-meter range. The full depth could be limited to a central part of the basin, for example a circular well. An alternative could be to utilise a tank facility that, for example, was previously used to store petroleum products. They have dimensions ideal for this purpose. However, water treatment and release of oil polluted water from such a facility would be challenging. Since such a facility is not known to us, experiments must be adapted to smaller facilities, and compromises need to be made.

Multiple experiments studying various aspects of subsea oil releases have been performed earlier in a six-meter high 42 m^3 large Tower Basin in Trondheim, Norway. These projects have focused on oil droplet formation, the effect of dispersant dosage and different injection techniques (Brandvik et al., 2018; Brandvik et al., 2019a). Related work has also been performed at other basin facilities in Canada (Belore, 2014), in France (Aprin et al., 2015) in China (Li et al., 2018) and in smaller scale at increased pressure (Malone et al., 2019; Malone et al., 2018; Aman et al., 2015; Brandvik et al., 2019b, 2019c).

* Corresponding author.
E-mail address: per.brandvik@sintef.no (P.J. Brandvik).

https://doi.org/10.1016/j.marpolbul.2020.111934
Received 2 June 2020; Received in revised form 5 December 2020; Accepted 8 December 2020
Available online 4 January 2021

After introducing the modified Weber scaling in 2013 (Johansen et al., 2013), generating additional laboratory data to further verify the algorithm over a wider range of release parameters has been a high priority. Availability to representative and high-quality datasets is vital for developing and verifying models for predicting oil droplet sizes. This paper describes a study that generated such a dataset by performing large-scale experiments at the US National Oil Spill Response Test Facility in New Jersey.

2. Experimental

The study presented in this paper was performed at Ohmsett, the US National Oil Spill Response Test Facility in New Jersey. It has proven to be very suited for testing of a broad range of oil spill technology where large-scale experiments can be performed due to the test tank dimensions (213 m, 21 m wide and 2.5 m deep). It has a unique capability to handle crude oil and an extensive oil removal/skimming and water filtration capability. Two movable bridges span the tank filled with 9500 m^3 of salt water. All experiments were performed with a water salinity of 2.75%. The reduced salinity is caused by freshwater input from precipitation. The water salinity is adjusted regularly by adding salt to the basin. No salt was added during this experimental period.

Simulating subsea releases in a basin with a depth of 2.5 m is not straight forward and multiple experimental approaches were evaluated, including both horizontal and vertical releases. To find the preferred experimental design, different releases were simulated with SINTEF's Plume3D model with an oil flow rate of 300 L/min (18 m^3/h) through a 30 mm orifice with different discharge arrangements (vertical and horizontal) and different towing speeds (0, 0.25 and 0.5 m/s), see Fig. 1. The results indicate that both horizontal and vertical discharge arrangement towed at a speed of 0.5 m/s may assure sufficient dilution ($n > 100$) at depths of about 1 m. However, the vertical discharge arrangement was preferred because the plume encountered a cross flow immediately causing more rapid dilution. This gave a shorter distance from the discharge point to the location where the dilution ratio exceeds 100:1 (less than 3 m, compared to 8 m for the horizontal discharge). Closer inspection of the results also reveals that the droplet separation is minimal for the vertical discharge – 99% of the oil remains in the plume at the distance where the dilution exceeds 100:1, while 30% of the oil has separated from the plume at the corresponding location for the horizontal discharge. This was probably caused by the greater entrainment of water, creating internal turbulence in the plume, for the vertical release.

The initial modelling (Fig. 1) led to performing a vertical release while moving the release point horizontally (simulating a horizontal cross current). This increased water entrainment gave sufficient dilution of the oil plume for monitoring the oil droplets, see Figs. 1 and S1 (Supplemental information). This was achieved by mounting both the release- and monitoring arrangements on two coordinated moving bridges, see Figs. 2 and S2. Two simultaneous series of oil releases were made during each experiment. The oil release points were at the bottom of the tank at positions dividing the width of the tank as shown in Figs. 2 and S1.

The oil and dispersant flow rates were monitored with inline flow meters and data acquisition systems. Typical flow rates (oil & dispersant) from the experiment and their uncertainty are presented in Fig. S3. Since Ohmsett is an outdoor facility, the experimental conditions were affected by the environmental conditions, especially outdoor temperature. Both water- and oil temperatures were monitored and used to calculate oil viscosities for the oil released in each experiment (Table 2 and Table 3). A summary of experiments performed during the test program is presented in Table 1. Totally nine experiments were performed, and three nozzle diameters were tested (25, 32 and 50 mm), each nozzle with a low, medium and high flowrate of oil, both with oil released alone (untreated) and oil treated with dispersant.

The towing speed, distance between bridges and instrument heights were adjusted to match the predicted trajectory of the oil plumes (taking into account oil release velocity and droplet sizes), see illustrations in Figs. S1, S2 and S4. Details regarding nozzle diameters, distances between bridges, positions of individual SilCams relative to the oil release and towing speeds used for each experiment are listed in Table S1. Further details can also be found in the technical report, Brandvik et al. (2017).

2.1. Oil and dispersant

Oseberg blend, also called Sture blend, was used to replicate work previously performed in the SINTEF Tower Basin (Brandvik et al., 2013). This blend is available from the Sture oil terminal outside Bergen, Norway. It is a light, paraffinic blend, with relatively stable composition and limited variation in properties. The batch used in this study (ID: 2015 0014) had a density of 0.826 g/mL (15.5 °C) and a viscosity of 5 mPa·s at shear rate 100 s^{-1} at the actual temperature for the testing 5 °C. A total volume of 12 m^3 was used in the nine experiments included in this study. Further details can be found in the technical report from this study, Brandvik et al. (2017).

Due to the large quantities needed, 200 litre of Corexit 9500 was transferred from a sealed 1000 litre pallet tank to a new plastic lined barrel and shipped to Ohmsett. The dispersant was injected through a T-joint on the oil supply pipe, located 6 release diameters (150–600 mm) before the oil release opening. This simulates injecting the dispersant with a wand inserted into the oil outlet. This technique is referred to as a "Simulated Insertion Tool" (SIT). Further details regarding different dispersant injection techniques are discussed in an earlier study (Brandvik et al., 2018).

2.2. IFT analysis

For the interfacial tension measurements by spinning drop method (Khelifa and So, 2009), the Dataphysics Spinning Drop Tensiometer

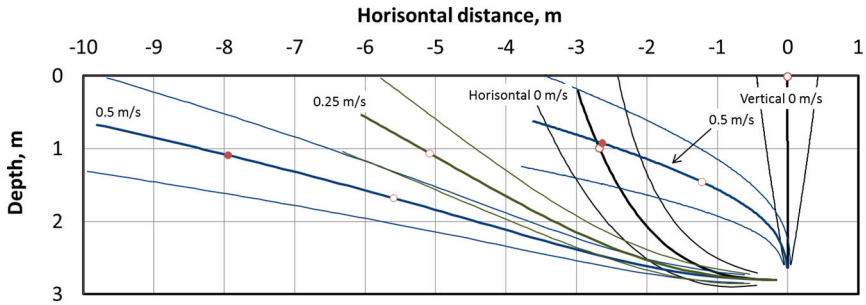

Fig. 1. Plume geometry computed for different discharge arrangements (vertical and horizontal) and towing speeds (0, 0.25 and 0.5 m/s from left to right). Open (filled) markers on the trajectories show the location where the dilution ratio exceeds 50:1 (100:1). The discharge rate is 300 L/min through an orifice diameter of 30 mm.

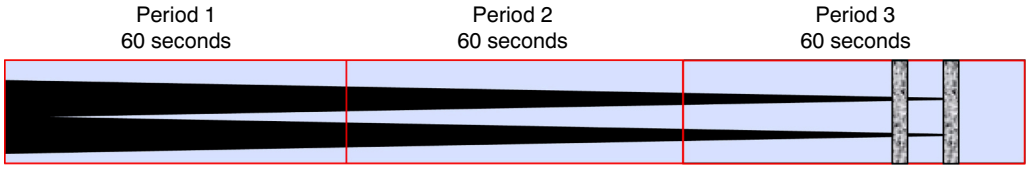

Fig. 2. Principle sketch of how one experiment in the Ohmsett basin was divided into periods with different oil flow rates, nozzle sizes and dispersant dosages.

SVT-20N with control and calculation software SVTS 20 IFT was used. Further details can be found in an earlier paper (Brandvik et al., 2013). IFT was in this study measured on premixed samples in the lab, not on samples taken in-situ in the basin during the experiments. Both oil and dispersant properties can vary significantly between batches and the combination of these batches of Oseberg blend and Corexit 9500 gave slightly lower interfacial tension values compared to earlier studies (Brandvik et al., 2019a). 1% dispersant resulted in an IFT of 0.2 mN/m.

2.3. Quantification of oil droplet sizes

Oil droplet sizes were quantified using a silhouette camera (SilCam). The SilCam operates using the principle of backlighting to create silhouettes of particles suspended between the light and the camera. Further details are given in Davies et al. (2017).

Two SilCam systems with different magnifications were used to optimize droplet sizing over the large range of diameters created during the experiments. Fifteen images were taken per second (approximately 4.5 GB of data generated per minute) and the number of droplets per image varies from 15 to several hundred, depending on the range of droplet sizes and resolution of the camera. The particle dimensions were quantified and used to determine droplet sizes and volume distribution. The number of droplets processed per distribution varied between around 20,000 for large untreated droplets to over 1 million for small droplets after dispersant treatment (see examples in Figs. 3, 5 and 7). A large difference in oil droplet sizes can visually be observed between the untreated and treated (1% 9500) oil droplets in these figures. This is a large advantage with the SilCam technology, that you have pictures to document the nature and size of the detected particles. The particle diameters were counted into log-spaced volume size classes, similar to the LISST-100 size classes. This enables a seamless transition in size distributions when comparing multiple magnifications and earlier results from the LISST-100. The objective was to position both SilCams within the oil plume during most of the experimental period. The predictions of the plume behaviour (Fig. S4) were used to position the SilCam in the plume. Examples of the oil droplet size distributions quantified by the upper and lower SilCams are given in Figs. S5, S6 and S7.

Table 1
Overview of large-scale experiments performed at Ohmsett.

Exp#	Nozzle (mm)	Flow rates (L/min)	Type of experiment	Oil volume (L)
1	25 32 50	50, 80, 120 80, 120 200, 300	Oil alone (untreated oil) - Low flow rate I	1545
2	25 32 50	80, 120 120, 300 300, 400	Oil alone (untreated oil) - High flow rate I	1773
3	25 32 50	50, 80, 120 120 200, 300	Dispersant injection (1%) - Low flow rate I	870
4	25 32 50	50, 80, 120 80, 120 200, 300	Oil alone (untreated oil) – Low flow rate II	1545
5	25 32 50	50, 80, 120 80, 300 400	Dispersant injection (1%) – High flow rate I	1030
6	25 32 50	50, 80, 120 120, 300 300, 400	Oil alone (untreated oil) – High flow rate II	2280
7	25 32 50	50, 80, 120 120 200, 300	Dispersant injection (1%) - Low flow rate II	870
8	32 32 50	80, 120, 300 – 200, 300, 400	Oil alone (untreated oil) – Various flow rates	2220
8	32 32 50	120 – 200, 300, 400	Dispersant injection – High flow rate II	1260
				12,193

3. Presentation and discussion of results

The main objectives with this study have been to generate a dataset that can fill the gap between earlier small-scale laboratory experiments (1–8 mm nozzle) studying subsea releases and the DeepSpill field experiment performed at 840 m depth outside Norway in 2000 (120 mm nozzle) (Johansen, 2003; Johansen et al., 2003; Chen and Yapa, 2003). The data from this study was generated mainly to verify models for oil droplet formation for subsea releases such as the modified Weber scaling (Johansen et al., 2013). Experiments were performed earlier at Ohmsett with a 25 mm nozzle (Zhao et al., 2016) but with very high release velocities to create sufficiently small oil droplets (<0.4 mm) to be quantified with available laser scattering technology (LISST-100).

The experimental data generated in this study represent more realistic range of oil droplet sizes, by using nozzles and oil flowrates giving lower exit velocities (1.7–6.2 m/s). These low velocities are more in line with real cases like Macondo (approx. 1 m/s). The volume median diameter (d_{50}) varied in this data from 1.2 mm to 5.8 mm for the untreated experiments and in the 0.20–0.40 mm range for oil treated with dispersant (1%). Representative oil droplet distributions for three oil flow rates (low/medium/high) for each of the three nozzle sizes tested (25, 32 and 50 mm) are presented in Figs. 4, 6 and 8. These figures also include oil size distributions for treated oil (1% dispersant) for the medium flow rates.

The results from the total of 9 experimental days (see Table 1) with two parallel releases and 3 or 4 different conditions (or time slots) for each experiment (Fig. 2), produced a wide table of results. The number of replicates for most combinations of nozzles and flow rates varied between 3 and 5. The experimental data is presented in Table 2 and Table 3. Totally, 53 different experiments are reported from this study.

3.1. Quality assurance of experiments

Not all experiments were successful, an evaluation of data quality of the droplet size data was based on several factors. The most significant were:

1. SilCam position in the plume: In some cases, we observed or experienced from the data that one or both instruments were not positioned correctly in the plume.
2. Smearing of optics: Smearing of the optics could occur, especially in experiments with the largest oil droplets.
3. Very high droplet concentration: In some cases, the plumes were too concentrated and reliable data could not be obtained.

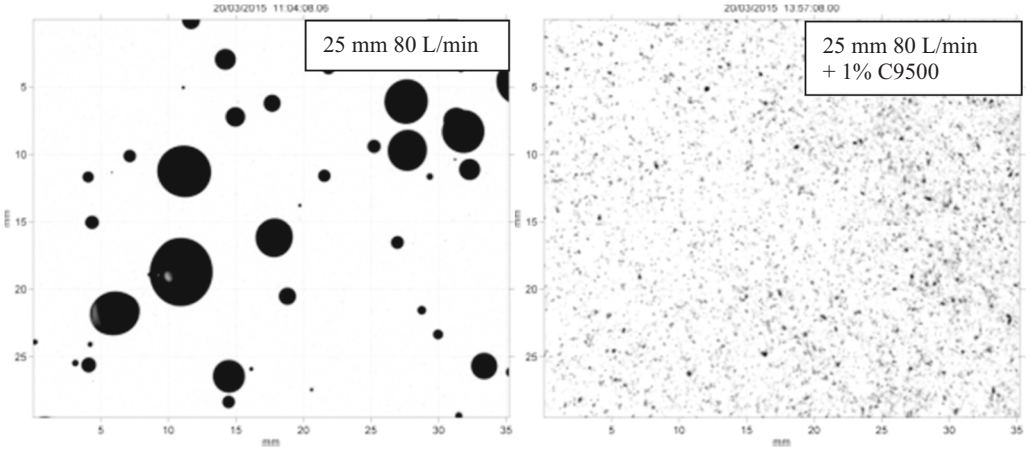

Fig. 3. SilCam images showing individual droplets (25 mm nozzle, 80 L/min and 80 L/min with 1% C9500).

4. Pump irregularities: All flow rates were monitored and documented with in-line flow meters (see example in Fig. S3). Oil and dispersant flow rates were generally very stable with standard deviations around 1%. However, larger deviations occurred, but were documented in the log-files.

Based on an evaluation of the factors described above, the quality of the individual replicate measurements was evaluated and 17% of the data were excluded due to documented conditions during the experiments. The excluded data are not reported in Table 2 and Table 3, but can be found in the technical report (Brandvik et al., 2017). Modified Weber scaling (Johansen et al., 2013) is used for the predicted droplet sizes in the tables (d_{50}), using coefficients A = 25 and B = 0.08 from Brandvik et al. (2014).

Correct positioning of the SilCams in the oil plume during the experiments was critical for measuring representative oil droplet sizes. Some oil droplet separation was observed in the rising oil plume as a function of oil droplet size (see Fig. S1). However, the experiments were designed to increase internal turbulence in the plume and reduce oil droplet separation, see Section 2 for further details. One SilCam was positioned in the upper part and one in the middle part of the rising oil plume. As expected, the upper SilCam measured slightly larger droplets than the lower Silcam. Examples in Figs. S5, S6 and S7 illustrate the deviation between the size distribution measured with the upper and lower instrument. The largest deviation was observed for experiments creating the largest droplets (low release velocities), due to the higher rising velocity of the large droplets. The droplet sizes (d_{50}) reported in Table 2 and Table 3 are averages from droplet distributions measured by both the upper and lower SilCam.

3.2. Oil droplet size versus nozzle size and flow rate

The results from these experiments can be sorted after the different nozzle sizes used 25 mm, 32 mm and 50 mm. Selected SilCam images

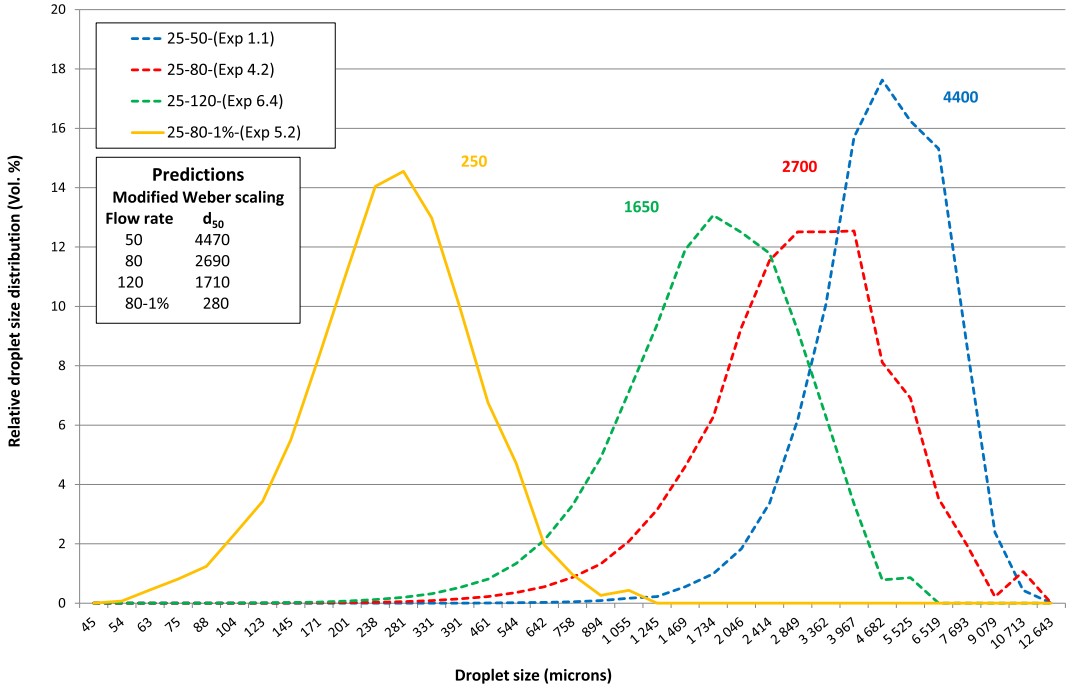

Fig. 4. Droplet size distribution (45–12,000 μm) from the experiments with the 25 mm nozzle at 50, 80 and 120 L/min and at 50 l/min with 1% Corexit 9500 (simulated injection tool – SIT). Numbers beside graphs are estimated d_{50} from cumulative distribution function (Upper SilCams). Average d_{50} (Upper and Lower SilCam) are found in Tables 2 and 3.

and oil droplet distributions from each of the three nozzle sizes are presented for 25 mm (Figs. 3–4), 32 mm (Figs. 5–6) and 50 mm (Figs. 7–8). These figures present selected oil droplet distributions for both oil alone and oil with dispersant injection. The droplet size distributions in these figures are from the Upper SilCams and the listed d_{50} are estimated from their cumulative distribution function. Averaged d_{50} (from both Upper and Lower SilCams) are found in Tables 2 and 3.

Replicate experiments were performed for each combination of nozzle size and flow rate, with an average of 5 replicates for oil alone experiments and 3 for experiments with dispersant injection, See technical report for further details (Brandvik et al., 2017). The scatter in the replicate data is illustrated for the 25 mm nozzle in Fig. S8 (oil alone experiments) and Fig. S9 (dispersant experiments). Standard deviation is in the 10–20% range for the untreated oil droplets and 5–20% for the droplets treated with 1% dispersant. The figures show that the average droplet sizes (circles) correspond well with predicted values (squares), both for untreated oil (Fig. S8) and for oil treated with dispersants (Fig. S9). Similar figures illustrating the experiments with the 32- and 50-mm nozzles can be found in the original technical report, see Brandvik et al. (2017).

The droplet size distributions for each flow rate & nozzle size generally show a good fit to a lognormal distribution. A possible improved fit to the more skewed Rosin Rambler can be seen for experiments with the largest oil droplets (lowest flow rates), where the largest bins represent a lower number of large and unstable droplets. The reduced stability of the largest droplets could distort the upper tail of the distribution. We are also approaching the upper detection range for the configuration of the SilCams used during these experiments. The optical path length for the SilCams used for the largest droplets was 12 mm.

3.3. Measured versus predicted particle sizes

One of the main objectives of this study was to generate droplet size data from up-scaled releases to improve or verify existing models for predicting initial droplet size distribution from subsea releases. The generated droplet data are more representative for real conditions with respect to lower release velocity (2–5 m/s) and larger droplet sizes (multiple millimeters). Modified Weber scaling (Johansen et al., 2013) is one of the alternatives for predicting initial droplet sizes from subsea releases. A summary of measured droplet sizes (d_{50}/D) for all experiments performed in this study and the DeepSpill experiment are plotted against modified Weber numbers in Fig. 9. Predicted d_{50} for versus measured d_{50} for averaged values are presented in Fig. 10 and for all the replicates in Fig. S10.

Table 2
Oil alone experiments: Droplet sizes (d_{50} - averaged from Upper and Lower SilCam) with varying nozzle size (25–50 mm), oil flow rates (50–400 L/min). Colour shadings for selected experiments correspond to colours used in Fig. 4 (25 mm), Fig. 6 (32 mm) and Fig. 8 (50 mm). Average values and estimates for uncertainty (rel. Standard deviation) are presented in Table S2 and in Fig. 10.

Exper. no	Nozzle (mm)	Flow rate (L/min)	Oil temp (°C)	Water temp (°C)	Calc. oil visc (mPa·s)	DOR %	IFT (mNM)	Measured d_{50} (µm)	Predicted d_{50} (um)
1.1	25	50	13	5.1	4.6	0	20	4450	4450
4.1	25	50	4.7	5.7	5.0	0	20	4150	4500
1.2	25	80	13	5.1	4.6	0	20	3450	2700
1.3	25	80	13	5.1	4.6	0	20	2950	2700
2.1	25	80	3.8	4.5	5.1	0	20	2700	2700
2.1	25	80	3.8	4.5	5.1	0	20	2350	2700
4.2	25	80	4.7	5.7	5.0	0	20	3050	2700
4.3	25	80	4.7	5.7	5.0	0	20	3150	2700
6.1	25	80	6	5.6	4.9	0	20	3000	2700
6.2	25	80	6	5.6	4.9	0	20	2050	2700
1.4	25	120	13	5.1	4.6	0	20	1600	1700
2.3	25	120	3.8	4.5	5.1	0	20	2300	1700
4.4	25	120	4.7	5.7	5.0	0	20	2000	1700
6.3	25	120	6	5.6	4.9	0	20	1450	1700
6.4	25	120	6	5.6	4.9	0	20	1750	1700
1.5	32	80	13	5.1	4.6	0	20	4650	4950
8.1	32	80	7	5.3	4.9	0	20	4700	4950
8.2	32	80	7	5.3	4.9	0	20	4150	4950
1.6	32	120	13	5.1	4.6	0	20	3300	3250
2.4	32	120	3.8	4.5	5.1	0	20	3350	3250
4.5	32	120	4.7	5.7	5.0	0	20	2700	3250
6.5	32	120	6	5.6	4.9	0	20	2400	3250
8.3	32	120	7	5.3	4.9	0	20	3350	3250
6.6	32	300	6	5.6	4.9	0	20	1350	1200
8.4	32	300	7	5.3	4.9	0	20	1700	1200
1.7	50	200	13	5.1	4.6	0	20	5200	5000[a]
4.6	50	200	4.7	5.7	5.0	0	20	3900	5000[a]
8.5	50	200	7	5.3	4.9	0	20	4550	5000[a]
1.8	50	300	13	5.1	4.6	0	20	3700	3700
4.7	50	300	4.7	5.7	5.0	0	20	2900	3700
8.6	50	300	7	5.3	4.9	0	20	3700	3700
6.7	50	400	6	5.6	4.9	0	20	2100	2700
8.7	50	400	7	5.3	4.9	0	20	3100	2700

[a]Predicted oil droplet sizes corrected for d_{max} ($d_{95} > d_{max}$), see Section 3.3 for further details.

Table 3
Experiments with dispersant injection: Droplet sizes (d_{50} - averaged from Upper and Lower SilCam) with varying nozzle size (25–50 mm) and oil flow rates (50–400 L/min). Colour shadings for selected experiments correspond to colours used in Fig. 4 (25 mm), Fig. 6 (32 mm) and Fig. 8 (50 mm). Average values and estimates for uncertainty (rel. Standard deviation) are presented in Table S2 and in Fig. 10.

Exper. no	Nozzle (mm)	Flow rate (L/min)	Oil temp (°C)	Water temp (°C)	Oil visc (mPa·s)	DOR %	IFT (mNM)	Measured d_{50} (µm)	Predicted d_{50} (um)
5.1	25	50	4.6	5.7	5.0	1	0.2	490	380[a]
7.1	25	50	5.8	5.6	5.0	1	0.2	500	380[a]
3.1	25	80	3.2	5.7	5.1	1	0.2	240	280
5.2	25	80	4.6	5.7	5.0	1	0.2	230	280
7.2	25	80	5.8	5.6	5.0	1	0.2	230	280
3.2	25	120	3.2	5.7	5.1	1	0.2	250	190
5.3	25	120	4.6	5.7	5.0	1	0.2	250	190
7.3	25	120	5.8	5.6	5.0	1	0.2	250	190
5.4	32	80	4.6	5.7	5.0	1	0.2	280	380[a]
7.4	32	80	5.8	5.6	5.0	1	0.2	540	380[a]
3.3	32	120	3.2	5.7	5.1	1	0.2	220	320
9.2	32	120	7	5.6	4.9	1	0.2	240	320
5.5	32	300	4.6	5.7	5.0	1	0.2	200	140
3.4	50	200	3.2	5.7	5.1	1	0.2	260	380[a]
9.4	50	200	7	5.6	4.9	1	0.2	210	380[a]
3.5	50	300	3.2	5.7	5.1	1	0.2	230	360
7.5	50	300	5.8	5.6	5.0	1	0.2	230	360
9.5	50	300	7	5.6	4.9	1	0.2	220	350
5.6	50	400	4.6	5.7	5.0	1	0.2	230	280
7.6	50	400	5.8	5.6	5.0	1	0.2	230	280

[a]Predicted oil droplet sizes corrected for d_{max} ($d_{95} > d_{max}$), see Section 3.3 for further details.

Experiments with untreated and treated oil are depicted with filled and open markers respectively (Fig. S10). The broken lines in the graph show the root relative mean square relative error (RMSE) which was found to be ±23% for the whole dataset. This may be compared to the relative standard deviations in volume median droplet diameters found in the replicate data sets, which was ±15%. The remaining error may be due to uncertainties in the physical properties of the oil (e.g. interfacial tension and oil viscosity), and unexplained factors in the prediction model.

The maximum stable diameter d_{max} of oil droplets is known to be limited by secondary breakup of droplets rising freely in water. This upper limit in droplet diameter is not covered in the Weber number scaling model and must be imposed by an additional calculation. In droplet breakup experiments with small outlet diameters, this limit was of no concern, but in the present study with much larger outlet diameters, we have found that the upper droplet diameter limit may be approached in certain cases. We have estimated d_{max} from a study presented by Hu and Kintner (1955). They found that the peak terminal rise velocity of an oil droplet U_P in water is depending on the physical properties of oil and water, as expressed by the following equation:

$$U_P = 1.23\,(\sigma/\mu_w)\,\mathrm{Mo}^{0.238}, \tag{1}$$

where σ is the interfacial tension between oil and water, μ_w is the dynamic viscosity of water, and Mo is Morton's number, $\mathrm{Mo} = g'\mu_w^4/\rho_w\sigma^3$. Here, $g' = g(\rho_w - \rho_{oil})/\rho_w$ is the reduced gravity, where ρ_w and ρ_{oil} are densities of water and oil, and g is the acceleration of gravity. The corresponding peak droplet diameter d_P can be estimated from the peak *droplet Weber number* $\mathrm{We}_d^{(P)} \approx 3$, where the droplet Weber number is given as $\mathrm{We}_d = \rho_w U_d^2 d/\sigma$, and U_d is the terminal rise velocity of the droplet of diameter d, i.e.

$$d_P = \mathrm{We}_d^{(P)} \Big/ \left(U_P^2\,\rho_w\right) \tag{2}$$

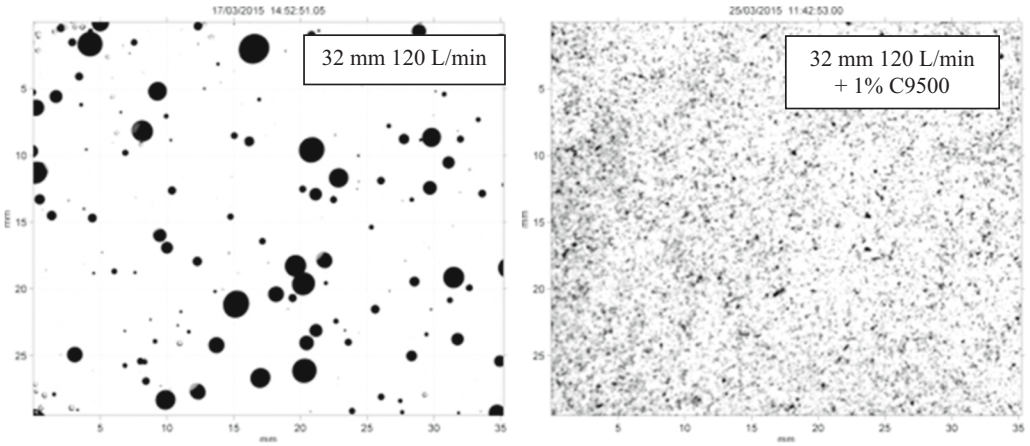

Fig. 5. SilCam images showing individual droplets (32 mm nozzle, 120 L/min and 120 L/min with 1% C9500).

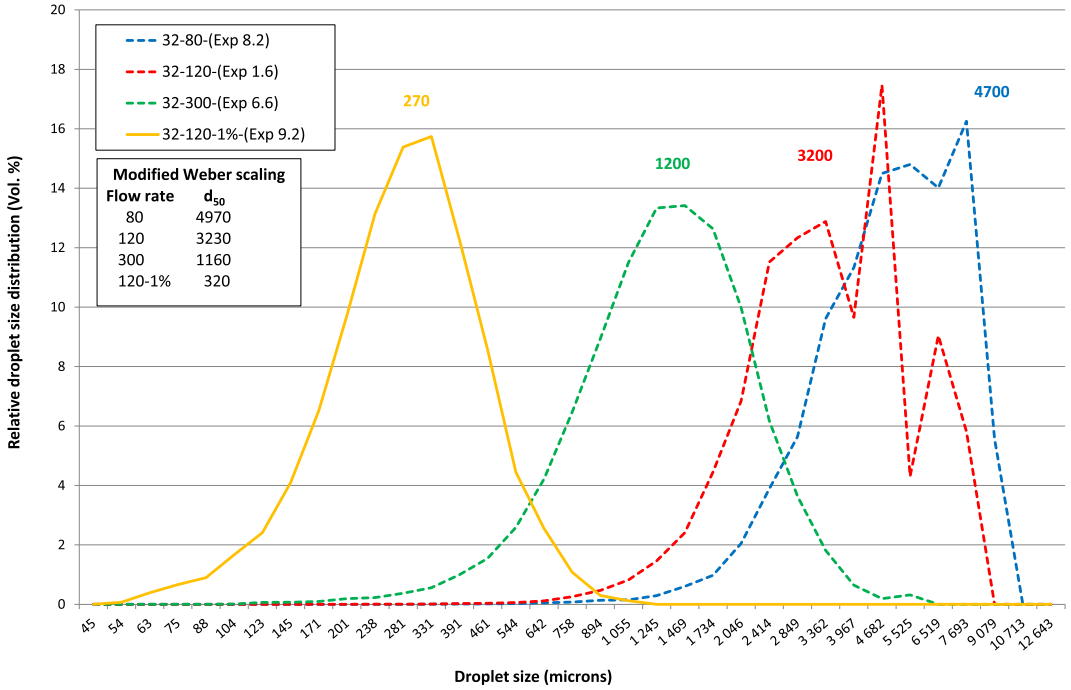

Fig. 6. Droplet size distribution (45–12,000 μm) from the experiments with the 32 mm nozzle at 80, 120 and 300 L/min and at 50 l/min with 1% Corexit 9500 (simulated injection tool – SIT). Numbers beside graphs are estimated d_{50} from cumulative distribution function (Upper SilCams). Average d_{50} (Upper and Lower SilCam) are found in Tables 2 and 3.

For untreated oil, the rise velocity is found to be nearly constant for droplet diameters greater than the peak diameter. This implies that the corresponding maximum stable droplet diameter $d_{\max}$ can be found from the critical droplet Weber number for secondary breakup. According to Hu and Kintner (1955), the critical droplet Weber number for secondary breakup is $We_d^{(C)} \approx 10$, which implies:

$$d_{\max} = d_P We_d^{(C)} \Big/ We_d^{(P)} \approx 3.3\, d_P. \quad (3)$$

In general, the peak droplet Weber number ($We_d \approx 3$) signals the onset of significant deformations of the droplet, causing increased drag forces. For untreated oil, this leads to stagnation in the terminal rise velocity of the droplet with further increase in the droplet diameter. However, for oil treated with dispersants, the rise velocity is found to continue to increase for droplet diameters greater than the peak diameter, but with a smaller slope than before the peak is reached: Calculations with the droplet rise model of Bossano and Dente (2009) indicate that the rise velocity after the peak will vary approximately as $U_d/U_P \approx (d/d_P)^{1/2}$ (see Fig. S11). This implies that the maximum stable droplet size $d_{\max}$ for treated oil can be found from the equation:

$$d_{\max} = d_P \left(We_d^{(C)} \Big/ We_d^{(P)} \right)^{1/2} \approx 1.8\, d_P \quad (4)$$

Thus, to avoid over-predictions of the droplet diameters with the Weber scaling model, we have compared the predicted d_{95} droplet size with $d_{\max}$, and if $d_{95} > d_{\max}$, d_{95} is set equal to $d_{\max}$. The d_{95} droplet size is related to the median droplet size d_{50} by a factor f_{95}, depending on the actual droplet size distribution, i.e. $d_{95} = f_{95} d_{50}$. Based on the droplet size distributions observed in this study, f_{95} is set to 2.6. In Tables 2 and 3, predicted droplet sizes (d_{50}) with application of this adjustment are marked with an asterisk (*). The tables show that this adjustment eliminates over-predictions in several cases for both untreated and treated oil. On this basis, we recommend that this adjustment should be utilised in conjunction with Weber number scaling predictions for real blowout conditions when the upper stable droplet diameter limit is even more likely to apply.

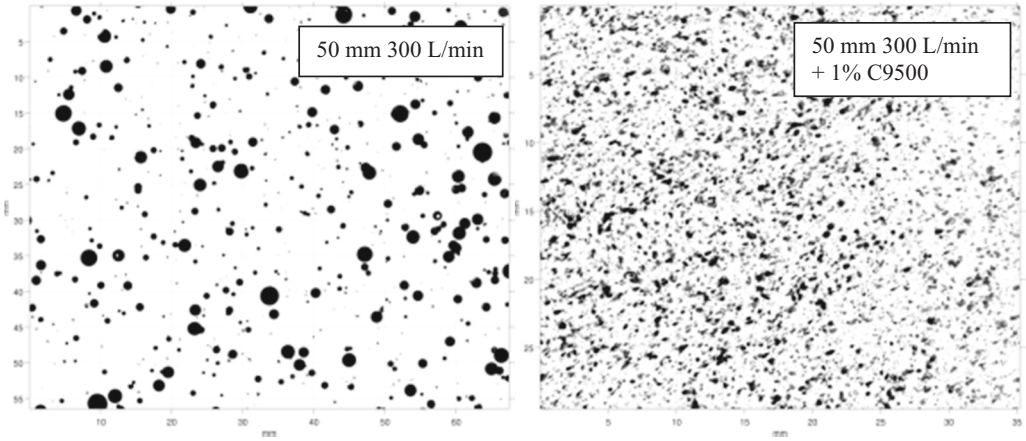

Fig. 7. SilCam images showing individual droplets (50 mm nozzle, 300 L/min and 300 L/min with 1% C9500). NB! Note the different scaling!

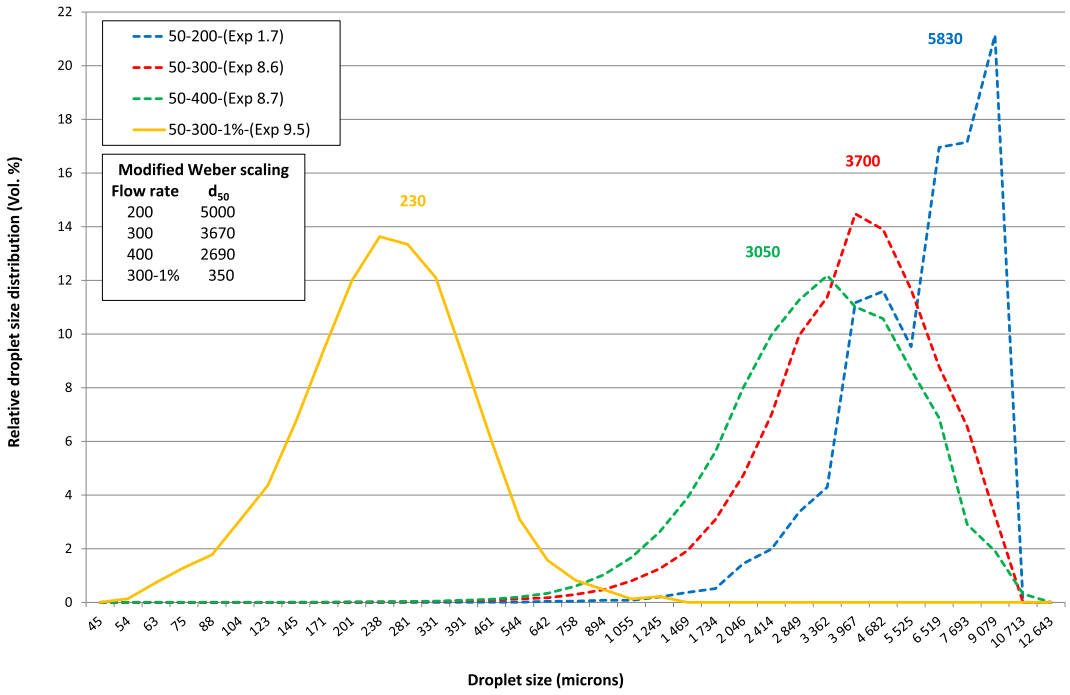

Fig. 8. Droplet size distribution (45–12,000 μm) from the experiments with the 50 mm nozzle at 200, 300 and 400 L/min and at 300 l/min with 1% Corexit 9500. Numbers beside graphs are estimated d_{50} from cumulative distribution function (Upper SilCams). Average d_{50} (Upper and Lower SilCam) are found in Tables 2 and 3.

4. Conclusions

The large-scale experimental data generated in this study represents more realistic release conditions, mainly lower release velocities (1.7–6.2 m/s) than earlier experiments. The oil droplet sizes produced for both treated oils (d_{50} of 200–400 μm) and for untreated oils (d_{50} of 1700–5200 μm) are more representative of realistic droplet sizes for a deep-water oil release. This study represents a major leap forward in generating experimental data for models predicting initial droplet sizes from subsea oil release and the effectiveness of subsea dispersant injection (SSDI). The experimental data generated in this study show a very high correlation with predicted values (see Figs. 9 and 10) from the modified Weber scaling algorithm ($r^2 = 0.95$). No bimodal oil droplet size distributions were observed in this extensive dataset.

The experiments show that SSDI will reduce the droplet size by an order of magnitude using a dispersant dosage of 1%. Since the untreated droplets formed in these experiments were similar in size to those expected in a real-world blowout like Macondo, the study results strongly suggest that SSDI would provide similar performance in the real world.

This new large-scale data set fills in the gap between the earlier SINTEF studies in the Tower Basin and Mini Tower and the DeepSpill field release in 2000, both with respect to release diameters, oil flow rates and droplet sizes. The data set is also unique with respect to its high number of replicate measurements (3–5 replicates for most settings).

The large oil droplets formed under these more realistic release conditions, the good fit with the DeepSpill field experiment and the high correlation with modified Weber scaling contradicts the very small oil droplet sizes reported from other simulated deep water releases (Paris et al., 2012; Aman et al., 2015; Malone et al., 2019). In these studies, small initial oil droplet sizes for full-scale subsea releases are also predicted, probably due to calibration coefficients that are not representative of the turbulence present in such releases. However, other scientists predict droplet sizes that correspond well with those reported in this study (Adams et al., 2013; Zhao et al., 2015; Testa et al., 2016; Cooper et al., 2020).

Also, a more recent large-scale study performed at Ohmsett, focusing on subsea releases of both oil and gas and dispersant injection, showed a high correlation between measured and predicted droplet sizes using modified Weber scaling (Ahnell et al., 2018; Davies et al., 2018).

CRediT authorship contribution statement

Per Johan Brandvik: Supervision, Project administration, Funding acquisition, Conceptualization, Data analysis, Writing.
Emlyn Davies: Methodology, Software, Instrumentation, Data analysis and Writing.
Frode Leirvik: Methodology, Instrumentation, and Data validation.
Øistein Johansen: Methodology, Data analysis and Writing.
Randy Belore: Conceptualization, Methodology, and Instrumentation.

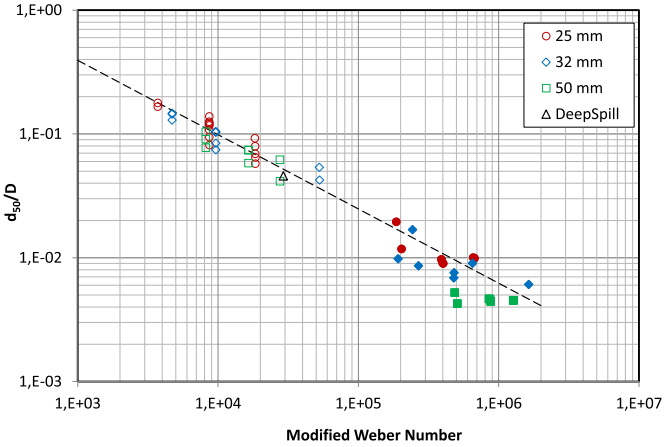

Fig. 9. d_{50}/D from experimental data plotted against the modified Weber number. Results are sorted after oil nozzle size. Filled symbols are experiments with dispersant injection; open symbols are experiments with untreated oil. The DeepSpill experiment from 2001 is also included (Johansen, 2003; Chen and Yapa, 2003). The dashed line represents the predicted line with coefficients A = 25 and B = 0.08, from Brandvik et al. (2014).

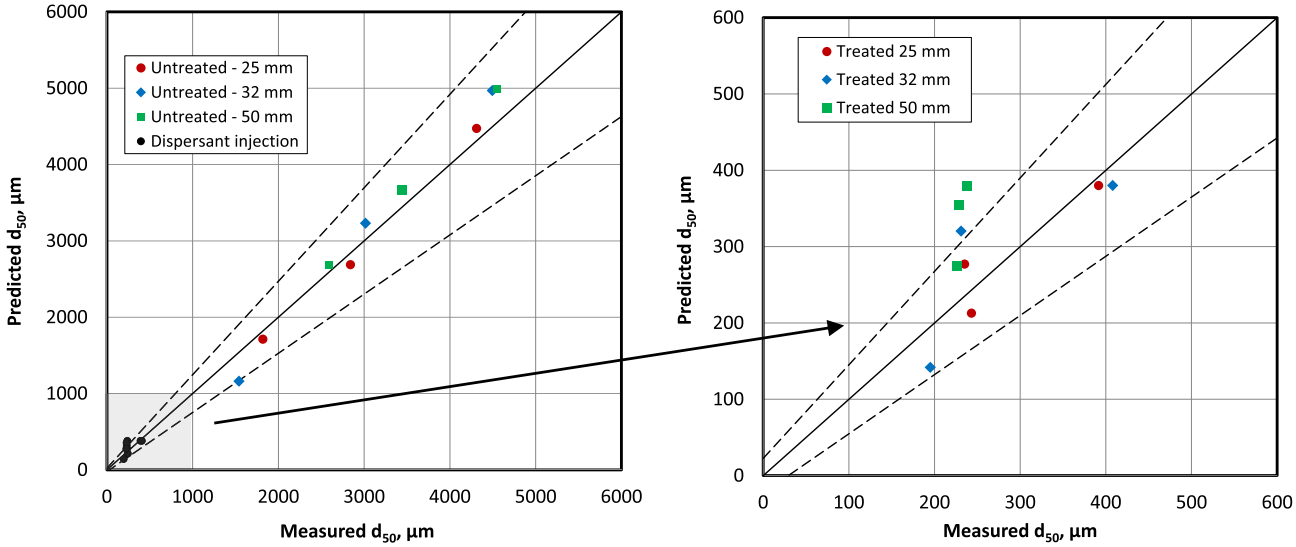

Fig. 10. Left figure: All average measured versus predicted oil droplet sizes ($r^2 = 0.95$). Dotted lines indicate ±15% deviation (sample STDev) from a perfect fit (solid line). Left figure contains all averaged samples. Right figure is zoomed in on treated (dispersant injection) samples only (grey rectangle in left figure). Figure presenting all replicates is presented as supplementary information (S10).

Declaration of competing interest

The authors declare that they have no known competing financial interests or personal relationships that could have appeared to influence the work reported in this paper.

Acknowledgement

Without the dedicated crew from MAR, led by Senior Test Engineer Allan Guarino, it would not have been possible to perform the high number of challenging experiments on the limited time available. This study was funded by the American Petroleum Institute, United States (API). The API Subsea Dispersant D3 steering committee members, Tim Nedwed, Cort Cooper and Oliver Pelz are thanked for valuable discussions and input during this work.

Appendix A. Supplementary data

Supplementary data to this article can be found online at https://doi.org/10.1016/j.marpolbul.2020.111934.

References

Adams, E.E., Socolofsky, S.A., Boufadel, M., 2013. Comment on "Evolution of the Macondo well blowout: simulating the effects of the circulation and synthetic dispersants on the subsea oil transport". Environ. Sci. Technol. 2013.

Ahnell, A., Davies, E., Brandvik, P.J., Leirvik, F., 2018. Optical Monitoring of Subsea Blowout Droplets and Subsea Dispersant Efficacy. Exponent Report for U.S. Department of the Interior Bureau of Safety & Environmental Enforcement (BSEE), p. 116 (ISBN: 1602129.000-5372).

Aman, Zachary M., Paris, Claire B., May, Eric F., Johns, Michael L., Lindo-Atichati, Davidi, 2015. High-pressure visual experimental studies of oil-in-water dispersion droplet size. Chemical Engineering Science 127, 392–400 (4 May).

Aprin, L., Heymes, F., Lauret, P., Slangen, P., Le Floch, S., 2015. Experimental characterization of the influence of dispersant addition on rising oil droplets in water column. Chemical Engineering Transaction 43, 2015. https://doi.org/10.3303/CET1543382.

Belore, R., 2014. Subsea chemical dispersant research. In: Proceedings of the 37th AMOP Technical Seminar on Environmental Contamination and Response. Canmore, Alberta, pp. 618–650.

Bossano, G., Dente, M., 2009. Single bubble and drop motion modelling. In: AIDIC Conference Series, vol. 9. https://doi.org/10.3303/ACOS0909007.

Brandvik, P.J., Johansen, Ø., Leirvik, F., Farooq, U., Daling, P.S., 2013. plet breakup in sub-surface oil releases – part 1: experimental study of droplet breakup and effectiveness of dispersant injection. Mar. Pollut. Bull 73 (1), 319–326.

Brandvik, P.J., Johansen, Ø., Farooq, U., Angell, G., Leirvik, F., 2014. Sub-surface Oil Releases – Experimental Study of Droplet Distributions and Different Dispersant Injection Techniques. A Scaled Experimental Approach Using the SINTEF Tower Basin – Version 2. SINTEF Report No: A26122. Trondheim Norway 2014, ISBN 9788214057393.

Brandvik, P.J., Davies, E., Johansen, Ø., Leirvik, F., Belore, R., 2017. Subsea Dispersant Injection – Large-scale Experiments to Improve Algorithms for Initial Droplet Formation (Modified Weber Scaling). An Approach Using the Ohmsett Facility, NJ, USA and SINTEF Tower Basin in Norway. SINTEF Report No: OC2017 A-087. Trondheim Norway 2017, ISBN 9788271742805.

Brandvik, P.J., Johansen, Ø., Leirvik, F., Krause, D.F., Daling, P.S., 2018. Subsea dispersants injection (SSDI), effectiveness of different dispersant injection techniques – an experimental approach. Mar. Pollut. Bull. 136, 385–393.

Brandvik, P.J., Daling, P.S., Leirvik, F., Krause, D.F., 2019a. Interfacial tension between oil and seawater as a function of dispersant dosage. Mar. Pollut. Bull. 143, 109–114.

Brandvik, P.J., Davies, E., Storey, C., Johansen, Ø., 2019b. Formation and quantification of oil droplets under high pressure down-scaled laboratory experiments simulating deep water releases and subsea dispersants injection (SSDI). Mar. Pollut. Bull. 138, 520–525.

Brandvik, P.J., Storey, C., Davies, E., Johansen, Ø., 2019c. Combined releases of oil and gas under pressure; the influence of live oil and natural gas on initial oil droplet formation. Mar. Pollut. Bull. 140, 485–492.

Chen, F.H., Yapa, P.D., 2003. A Model for Simulating Deepwater Oil and Gas Blowouts - Part II: Comparison of Numerical Simulations With "Deepspill" Field Experiments.

Cooper, C., Adams, E., Gros, J., Socolofsky, S., 2020. An Evaluation of Models to Calculate Droplet Size From Subsurface Oil Releases (in preparation).

Davies, E.J., Brandvik, P.J., Leirvik, F., Nepstad, R., 2017. The use of wide-band transmittance imaging to size and classify suspended particulate matter in seawater. Mar. Pollut. Bull 115, 105–114.

Davies, E.J., Ahnell, A., Leirvik, F., Brandvik, P.J., 2018. Optical monitoring of subsea blowout droplets and subsea dispersant efficacy. Proceedings of the Forty-first AMOP Technical Seminar, Environment and Climate Change Canada, Ottawa, ON, Canada, pp. 90–111.

Hu, S., Kintner, R.C., 1955. The fall of single liquid drops through water. A.I.Ch.E. Journal 1, 42–48.

Johansen, Ø., 2003. Development and verification of deep-water blowout models. Mar. Pollut. Bull. 47, 360–368.

Johansen, Ø., Rye, H., Cooper, C., 2003. Deep spill – field study of a simulated oil and gas blow-out in deep water. Spill Science & technology Bulletin 8, 433–443.

Johansen, Ø., Brandvik, P.J., Farooq, U., 2013. Droplet breakup in sub-surface oil releases – part 2: predictions of droplet size distributions with and without injection of chemical dispersants. Mar. Pollut. Bull 73 (1), 327–335.

Khelifa, A., So, L.L.C, 2009. Effects of chemical dispersants on oil-brine interfacial tension and droplet formation. In: 32nd AMOP Techn. Seminar, pp. 383–396.

Li, Z., Spaulding, M.L., French McCay, D., Crowley, D., Payne, J.R., 2017. Development of a unified oil droplet size distribution model with application to surface breaking waves and subsea blow-out release considering dispersant effects. Mar. Pollut. Bull. 114 (1), 247–257.

Li, J., An, W., Gao, H., Zhao, Y., Sun, Y., 2018. An experimental study on oil droplet size distribution in subsurface oil releases. Acta Oceanol. Sin. 37, 88–95. https://doi.org/10.1007/s13131-018-1258-5.

Malone, K., Pesch, S., Schluter, M., Krause, D., 2018. Oil droplet size distributions in deep-sea blow-outs: influence of pressure and dissolved gases. Env. Sci. & Tech. https://doi.org/10.1021/acs.est.8b00587.

Malone, K., Aman, Z.M., Pesch, S., Schluter, M., Krause, D., 2019. Jet formation at the spill site and resulting droplet size distributions, chapter 4. In: Murawski, et al. (Eds.), Deep Oil Spills. Springer. https://doi.org/10.1007/978-3-030-11605-7.

NASEM (National Academies of Sciences, Engineering, and Medicine), 2019. The Use of Dispersants in Marine Oil Spill Response. The National Academies Press, Washington, DC. https://doi.org/10.17226/25161.

Nissanka, I.D., Yapa, P.D., 2016. Calculation of oil droplet size distribution in an underwater oil well blow-out. J. Hydr. Res. https://doi.org/10.1080/00221686.2016.1144656.

Nissanka, I.D., Yapa, P.D., 2018. Calculation of oil droplet size distribution in ocean oil spills: a review, Marine. Poll. Bull. 135, 723–734. https://doi.org/10.1016/j.marpolbul.2018.07.048.

Paris, C.B., le Henaff, M., Aman, Z.M., Subramaniam, A., Helgers, J., Wang, D.P., Kourafalou, V.H., Srinivasan, A., 2012. Evolution of the Macondo well blowout: simulating the effects of the circulation and synthetic dispersants on the subsea oil transport. Environ. Sci. Technol. 46, 13293–13302.

Pesch, S., Jaeger, P., Malone, K., Paris, C., Aman, Z., Krause, D., Hoffmann, M., Schluter, M., 2019. Experimental investigation of deep-sea oil spills under in-situ conditions: influence of high pressure and turbulent multiphase flow, Proc. In: 10th Inter. On Multiphase Flow, Conf.

Socolofsky, S., Adams, E., Boufadel, M., Aman, Z., Johansen, Ø., Konkel, W., Lindo, D., Madsen, M., North, E., Paris, C., Rasmussen, D., Reed, M., Rønningen, P., Sim, L., Uhrenholdt, T., Anderson, K., Cooper, C., Nedwed, T., 2015. Intercomparison of oil spill prediction models for accidental blowout scenarios with and without subsea chemical dispersant injection. Mar. Pollut. Bull. 2015, 110–126.

Testa, J.M., Adams, E., North, E.W., He, R., 2016. Modeling the influence of deep water application of dispersants on the surface expression of oil: a sensitivity study. J. Geophys. Res. Ocean. 121, 5995–6008.

Zhao, L., Boufadel, M.C., Socolofsky, S.A., Adams, E., King, T., Lee, K., 2014. Evolution of droplets in subsea oil and gas blow-outs: development and validation of the numerical model VDROP-J. Mar. Pollut. Bull. 83 (1), 58–69.

Zhao, L., Boufadel, M.C., Adams, E., Socolofsky, S.A., King, K., Lee, K., Nedwed, T., 2015. Simulation of scenarios of oil droplet formation from the Deepwater Horizon blowout. Mar. Pollut. Bull. 304–319.

Zhao, L., Shaffer, Franklin, Robinson, Brian, King, Thomas, D'Ambrose, Christopher, Pan, Zhong, Gao, Feng, Miller, Richard S., Conmy, Robyn N., Boufadel, Michel C., 2016. Underwater oil jet: hydrodynamics and droplet size distribution. Chem. Eng. J. 299, 292–303.

Zheng, L., Yapa, P.D., Chen, F.H., 2003. A model for simulating deepwater oil and gas blowouts - part I: theory and model formulation. Journal of Hydraulic Research, IAHR 41 (4), 339–351 (August).